Validation of, and limitations on, the use of NEC-4 for radiation from antennas buried within a homogeneous half-space

David B. Davidson and H. du Toit Mouton
Department of Electrical and Electronic Engineering
University of Stellenbosch, Stellenbosch 7600, South Africa
E-mail: davidson@firga.sun.ac.za.

Abstract— **The use of the computer program NEC-4 for the simulation of radiation from buried antennas is considered. NEC-4 uses the "exact" Sommerfeld integral formulation for stratified media (in NEC-4, restricted to an homogeneous half-space). Although the formulation is rigorous, certain approximations have to be made for numerical implementation. The formulation, and some of these issues, are outlined in the paper. Several validation examples comparing results computed using NEC-4 and results available in the literature are presented for antennas buried in various typical media, including ground, fresh water and the sea. Satisfactory agreement has generally been obtained; where differences have been noted, we have able to explain most in terms of approximate implementation issues.**

Keywords— **Buried antennas; NEC-4; radiation; Sommerfeld integrals; validation**

I. Introduction

Wire antennas or scatterers buried in the ground or immersed in water are an important class of antenna. Applications are legion, and include communication with submarines, detection of buried pipes and other metallic objects, grounding stakes for HF antennas, and "hardened" antennas buried just below the surface of the ground to protect against nearby explosions. That this is still a topic of current interest is clear from recent work in France [1] on VLF antennas immersed in sea water. The classical approach (epitomized by King [2]) concentrated on Hertzian dipoles and used the Sommerfeld potentials. Recent versions of the Numerical Electromagnetics Code - Method of Moments Versions 3 and 4 (NEC-3 and 4) permit modelling of such buried antennas [3], [4] and this paper describes validation work of these capabilities that we have undertaken. In the rest of this paper, we will refer only to NEC-4 since this is the most recent, documented release. (The specific version used was NEC-4.1). NEC-2, now readily available in the public domain, also contains a Sommerfeld treatment for wires, but the formulation restricts wires to be *above* the air/ground interface. This restriction was removed in the subsequent releases described above. The theory on which NEC-4 rests is openly available [5] but we caution that the NEC-4 code itself has restricted distribution.

The organisation of this paper is the following. Firstly, an outline of the Sommerfeld formulation will be presented. Two different approaches are encountered in the literature, and we present a brief summary of both, before discussing the formulation used by NEC-4. It is useful for users to have an appreciation of the numerical integration used for near-field evaluation, and the uniform asymptotic approximations used for far-field evaluation, along with the problems associated with these, and we briefly review the approaches used by NEC-4. Then the numerical tests will be described, and an extensive comparison made of radiated field strength in several different media with analytical data available in the literature. The agreement is in general quite satisfactory, but there are some significant points of difference.

The main contributions of this paper are twofold: firstly, an evaluation of the accuracy of NEC-4 for fields at distances ranging from very near to quite far from antennas located just below the surface of representative media; and secondly, prominently highlighting the limitations of NEC-4 for such applications. Although the latter are discussed in the theory manual [3], the implications may not be immediately clear to the users without extensive experience with Sommerfeld integrals.

It should be noted that the conventional $1/r$ decay in free space is modified substantially in stratified, lossy media; hence, field strength vs. distance plots generally need to be computed for each combination of frequency and media. Although extensive validation results were reported in [5], these were all near-field results, concentrating on impedance and current distributions. Since we are comparing results computed using NEC-4 to published results in the literature which *also* use the Sommerfeld formulation — albeit for infinitesimal dipoles — the term "validation" in this paper should be understood to refer to the *implementation* of the formulation in NEC-4.

II. Overview of the Formulation

There are two approaches to the formulation of the Sommerfeld integrals. One uses vector potentials, and the basic approach follows rather elegantly from the solution of the wave equation in the spectral domain. The other approach uses dyadic Green's functions and the Sommerfeld integral identity.

A. Vector potential-based approach

In this section the theoretical background to the problem of an infinitesimal dipole near a planar interface is briefly discussed.

Figure 1 is a diagram of a short vertical and horizontal dipole near a planar interface. It is assumed that both mediums are non-magnetic in nature and there is no source of free charge except for a current element denoted by $\mathbf{J}_u$ at a height h above the surface. The differential equation for the magnetic vector potential $\mathbf{A}$ in both regions is given by:

$$\nabla^2\mathbf{A} + k^2\mathbf{A} = -\mu_o\mathbf{J}, \tag{1}$$

where k is the wave number in the specific medium. To exploit the two-dimensional rotational symmetry, the two-dimensional Fourier transform $\overline{\mathbf{A}}$ of $\mathbf{A}$ is calculated:

$$\overline{\mathbf{A}}(\beta_x, \beta_y, z) = \frac{1}{4\pi^2}\int_{-\infty}^{\infty}\int_{-\infty}^{\infty}\mathbf{A}e^{j(\beta_x x+\beta_y y)}\,dx\,dy. \tag{2}$$

This results in

$$\left(\frac{\partial^2}{\partial z^2} - \gamma^2\right)\overline{\mathbf{A}} = \mu_0\overline{\mathbf{J}}. \tag{3}$$

The following two boundary conditions apply at the interface between the two media:

- The magnetic vector potential is continuous everywhere, in particular at the interface between the two media.
- By making use of the Lorenz gauge condition it follows that

$$\frac{\nabla\cdot\overline{A}|_{z=0+}}{\nabla\cdot\overline{A}|_{z=0-}} = \frac{\epsilon_1}{\epsilon_2}. \tag{4}$$

These two conditions, together with the fact the magnetic flux density $\mathbf{B}$ is a continuous function, results in unique solutions to eqn. (3).

The basic strategy to solve the $\mathbf{E}$ and $\mathbf{H}$ fields is as follows:

1. The two-dimensional Fourier transform of $\mathbf{A}$ is calculated by solving eqn. (3) and making use of the boundary conditions. For a vertical dipole $\overline{\mathbf{A}}$ only has a nonzero z-component, while $\overline{\mathbf{A}}$ in general has nonzero z and x components for a horizontal dipole.

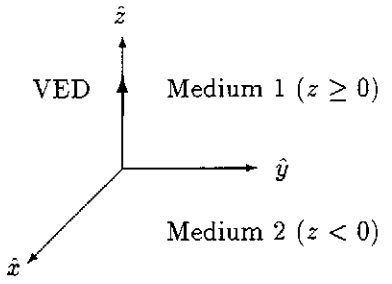

Vectical Electric Dipole (VED)

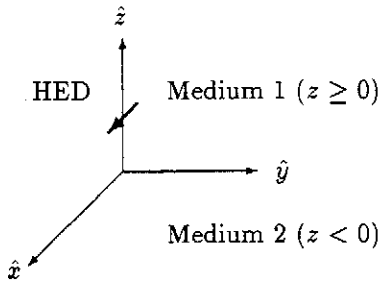

Horizontal Electric Dipole (HED)

Fig. 1. Short vertical and horizontal dipoles near a planar interface.

2. The inverse Fourier transform of $\overline{\mathbf{A}}$ is calculated. This leads to the well-known Sommerfeld integral which can in general only be solved numerically. We return to this in the following section. However, by making use of complex analysis (in particular the theory of branch cuts and Cauchy's theorem) some general conclusions can be made concerning the surface waves: At the boundary the z-component A_z of $\mathbf{A}$ consists of three components

$$A_z = Q_p + Q_1 + Q_2, \tag{5}$$

which are associated with three singularities in the Sommerfeld integral. Q_p gives rise to the so-called Zenneck surface wave — we return to this subsequently. Were it present, the Zenneck surface wave would decrease with $\rho^{-\frac{1}{2}}$. Q_1 is associated with a singularity at $-k_1$ in the Sommerfeld integral and results in the Norton surface wave. This wave decreases with $\frac{1}{\rho}$. Q_2 is associated with a singularity at k_2. The surface wave associated with this singularity decreases significantly faster than that of Q_1. (We also return to these waves in § III-B).

3. Once the magnetic vector potential is known the $\mathbf{E}$ and $\mathbf{H}$ fields can easily be calculated from the relations $\mathbf{B} = \mu\mathbf{H} = \nabla\times\mathbf{A}$ and $j\omega\epsilon\mathbf{E} = \nabla\times\mathbf{H}$.

A very readable outline of the procedure for a vertical electric dipole (VED) may be found in Collin [6];

however, the complexities of the integration required by the Sommerfeld integrals are not covered in detail. The derivation for the horizontal electric dipole (HED) is rather more complex than for the VED and was not readily available in the literature we consulted; a derivation may be found in [7].

B. Dyadic Green's function approach

This is essentially the approach used by NEC-4 — it might also be called the "field oriented" approach. Chew presents a very extensive discussion of this formulation [8, Chapter 2], from which the following is abstracted. (Note that Chew uses the $e^{-i\omega t}$ time convention. The necessary substitution $\pm i \rightarrow \mp j$ has been made in the following.) The geometry of Fig. 1 applies again in this section; the interfaces between different strata lie on planes on constant z. For the VED in Fig. 1, the TM component of the field is given by [8, eqn.(2.3.3a)]:

$$E_z = \frac{-j\omega\mu I\ell}{4\pi k^2}(k^2 + \frac{\partial^2}{\partial z^2})\frac{e^{-jkr}}{r} \tag{6}$$

Here, $I\ell$ is the current moment. Note that Chew uses the convention TM_z. Now, the Sommerfeld identity is introduced [8, eqn.(2.2.30)]:

$$\frac{e^{-jkr}}{r} = -j\int_0^\infty \frac{k_\rho}{k_z} J_0(k_\rho\rho)e^{-jk_z|z|}dk_\rho \tag{7}$$

J_0 is the Bessel function of first kind, order 0. The physical interpretation of the Sommerfeld identity is that a spherical wave can be expanded as an integral summation of conical waves or cylindrical waves in the ρ direction [8, p.66]. This identity, eqn. (7), is now substituted — in slightly modified form — into eqn. (6) to yield [8, eqn. (2.3.4)]:

$$E_z = \frac{-I\ell}{8\pi\omega\epsilon}\int_{-\infty}^\infty \frac{k_\rho^3}{k_z} H_0^{(1)}(k_\rho\rho)e^{-jk_z|z|}dk_\rho \tag{8}$$

This expression expands E_z as a superposition of cylindrical waves in the ρ direction, and plane waves in the z direction. Hence, the various strata result in reflection and transmission of the plane waves propagating in $\pm z$, and the appropriate coefficients follow from simple plane wave theory.

This plane wave insight is one of the major attractions of this formulation, and renders multi-layered media tractable. As an example, the field in region 1 (air in NEC-4) for a dipole located at height $z = d_1$ over an interface at $z = 0$ can be written as [8, eqn. (2.3.5)]:

$$E_{z_{11}} = \frac{-I\ell}{8\pi\omega\epsilon}\int_{-\infty}^\infty \frac{k_\rho^3}{k_{1z}} H_0^{(1)}(k_\rho\rho)\cdot [e^{-jk_{1z}|z|} + \tilde{R}_{12}^{TM}e^{-jk_{1z}z-2jk_{1z}d_1}]dk_\rho \tag{9}$$

where $k_{1z} = \sqrt{k_1^2 - k_\rho^2}$, k_1 is the wavenumber of the upper medium (k_0 in NEC-4), and the ij subscript on E_z indicates the source and field points are located in medium i and j respectively. The Fresnel reflection coefficient for the air/medium interface is given by [8, (2.1.14a)]

$$R_{12}^{TM} = \frac{\epsilon_2 k_{1z} - \epsilon_1 k_{2z}}{\epsilon_2 k_{1z} + \epsilon_1 k_{2z}} \tag{10}$$

For a source embedded in region 2, with the interface at $z = 0$, the field in region 1 is the field transmitted through the interface. The z dependence is thus $\sim e^{jk_{2z}z'}T_{12}^{TM}e^{-jk_{1z}z}$ for $z' < 0$ and $z > 0$. Noting that (from [8, eqn. (2.1.14b)], with the indices interchanged in this case):

$$T_{21}^{TM} = \frac{2\epsilon_1 k_{2z}}{\epsilon_1 k_{2z} + \epsilon_2 k_{1z}} \tag{11}$$

and that the k_z term in eqn. (8) is that of the medium surrounding the source, we find that

$$E_{z_{21}} \sim \int_{-\infty}^\infty k_\rho^3 H_0^{(1)}(k_\rho\rho)\cdot \frac{e^{jk_{2z}z'-jk_{1z}z}}{\epsilon_1 k_{2z} + \epsilon_2 k_{1z}}dk_\rho \tag{12}$$

where the constants have been dropped for clarity. This expression is consistent with [8, eqn.(2.4.15)], once the necessary simplifications are made for the two-media case.

The Sommerfeld potentials listed in the NEC-4 documentation [3, p.35] appear somewhat different, but this is simply due to notation. As an example, consider the following expression [3, eqn(5-7b),p.35], which represents the same field as eqn. (12):

$$E_{z12}^V(\rho, z) \sim \int_0^\infty \frac{e^{\gamma_1 z' - \gamma_2 z}}{k_1^2\gamma_2 + k_2^2\gamma_1}\cdot J_0(\lambda\rho)\lambda^3 d\lambda \tag{13}$$

Noting the differences in notation and convention (for instance, NEC-4 and Chew interchange the medium numbering, and the wavenumbers have the relationship $k_1 z = \pm j\gamma_2$), it is clear that these capture the same physics. A summary of the corresponding notation is given in Table I.

III. Evaluation of the Sommerfeld Potentials

The Sommerfeld potentials cannot be evaluated in closed form, and numerical integration is required. For even the simplest case of a homogeneous half-space, as

Parameter	Chew's notation	NEC-4
Integration variable	k_ρ	λ
Medium # & properties	Upper medium – # 1(arbitrary)	Upper medium – # 2 (air)
Wavenumber in z	$k_1 z = \sqrt{k_1^2 - k_\rho^2}$	$\gamma_2 = \sqrt{\lambda^2 - k_2^2}$

TABLE I
CORRESPONDING NOTATION: CHEW [8] AND NEC-4 [3].

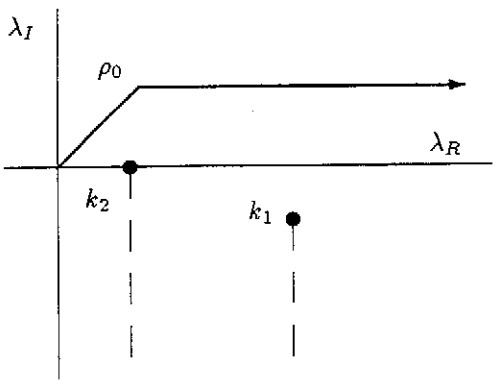

Fig. 2. Contour for evaluation of the Bessel function form of the Sommefeld integrals. The breakpoint and two branch cuts are shown; details of the selection of the breakpoint may be found in [3, §5.1.2].(After [3, Fig. 5-2]).

treated in NEC-4, there are numerous problems associated with this integral. The square root function in the terms γ_1 and γ_2 is double-valued, and it is necessary to use Riemann sheets to produce a continuous function [8, §2.2.3]. A Riemann sheet is demarcated by a branch cut, and in the present case there are two. Furthermore, there is a pole at $\lambda_p = \frac{k_1 k_2}{\sqrt{k_1^2+k_2^2}}$, which may lie on the real axis (the integration path) for lossless media. Finally, for large distances, the kernel exhibits rapid oscillations, requiring asymptotic evaluation using techniques such as the methods of stationary phase or steepest descent.

Although elegant and computationally efficient approaches are possible in particular regions, a *general purpose* program such as NEC-4 has to make certain approximations in the evaluation of these integrals. NEC-4 uses two different strategies to evaluate these integrals, valid in the near- and far-fields respectively.

A. Near-field numerical integration

For the near fields, NEC-4 builds up a table of Sommerfeld integrals for the particular frequency and material properties specified, using numerical integration. Interpolation is then used to compute fields as required when the impedance matrix is constructed. The integration path (along the real axis) is deformed into the upper half plane for $\lambda_R > 0$, to avoid the branch cuts; see Fig. 2. (Special care is required when the ratio of height to radial separation becomes small, and a Hankel function form of the integrals is then used.) This approach is used for separations up to of the order of a wavelength — the precise limits may be found in [3, p.41]. NEC-4 also includes a treatment for larger separations, using a model based parameter fit to a form suggested by the asymptotic one, to reduce the number of interpolation points required. Again, the precise limits are given in [3, p.44]. The range of validity of the numerical integration scheme in NEC-4 is $10^{-5} < k_2 R < 200$ [3, p.39], but these limits are not exploited by the code, which switches to an asymptotic approximation long before the upper limit is reached.

B. Far-field asymptotic approximation

For far-fields, a uniform asymptotic approximation is used. Although the simulations to be shown exercise primarily the near-field abilities of NEC-4, it is useful to also be aware of some limitations as regards the far-field implementation. The asymptotic approximation used incorporates second-order terms for the saddle point [8, p.82], [3, eqn. (5-18),p.48] near $k_2 = k_0$; note the use of the NEC-4 media numbering in this section. As the depth or height approach zero, so this saddle point approaches k_2. Similar second-order term as also used for the nearby pole at $\lambda_p = \frac{k_1 k_2}{\sqrt{k_1^2+k_2^2}}$. This saddle point and pole have the following respective interpretations [9]:

Source & field points above ground Represents the reflected ray; and the Norton surface wave. (The latter decays as $1/\rho$).

Source buried, field below ground Represents the ray going up to the interface, through the air and back into the ground; and the Norton surface wave.

Source buried, field above ground Represents the ray going up to the interface and mostly through air; and the Norton surface wave.

The other saddle point near k_1 (again, for zero height/depth, it is *at* k_1) has the following interpretation:

Source & field above ground Represents the *lateral* or *head* wave going into the ground, traveling through the ground, emerging again into the air near the field point. (See Fig.3; note the use of Chew's notation here). Note that this wave decays asymptotically as $1/\rho^2$.

The asymptotic approximation of this second saddle point is only first-order, with the result that it converges more slowly and goes to zero as the ray path

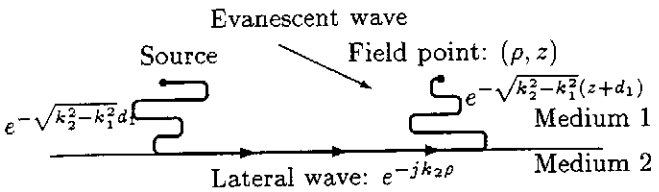

Fig. 3. Physical interpretation of the lateral wave. (After [8, Fig. 2.6.3]).

approaches grazing incidence on the interface. Thus the lateral wave is lost. For source and field points below ground, the field reflected from below the interface will be exactly cancelled by the direct field as the interface is approached — the "missing" lateral wave being required in this situation for a complete solution. For ground with any significant loss, the wave propagating through the ground is rapidly attenuated and the errors should not be significant. For source and field points located deeper below the interface, the below-ground wave becomes more accurate. Although a uniform two-saddle-point-and-pole approximation would address these issues, the existing single-saddle-point-and-pole approximation is already rather complex [9]. Note that these issues are only germane to the asymptotic approximation — for near-field data, the numerical solution is complete.

Chew discusses the various field species and their connection with the branch- and saddle points further in [8, §2.6.4]).

There has been some controversy regarding the contribution of the pole; it is known as the Sommerfeld or Zenneck surface wave pole [8, p.99], [9]. For two-layered media problems, it appears that the pole does not represent a true surface wave. (Of course, for multi-layered media, or two layered media with a ground, such as a microstrip structure, proper surface waves can be excited).

IV. Numerical tests

In order to validate the ground handling capabilities of the new NEC-4 code it was decided to compare results from the literature with independent NEC-4 simulations. Results for antennas in matter are rather sparse; the best sources are the monographs of King et al.'s [2] and Maclean and Wu [10].

The problem to be considered is that of an infinitesimal vertical or horizontal electric dipole near a planar interface. For a dipole buried in a particular medium one has to be careful in choosing its length. In a conducting medium, the wavelength-related parameter λ_c that should be used in determining segment sizes is [4, p.12]

$$\lambda_c = 299.8/(|\eta| f_{\mathrm{MHz}}), \tag{14}$$

with

$$|\eta| = \left[\epsilon_R^2 + 3.23(10^8)\left(\frac{\sigma}{f_{\mathrm{MHz}}}\right)^2\right]^{\frac{1}{4}}. \tag{15}$$

Note that the second part of eqn. (15) can easily overwhelm the first part in ϵ_R with highly conductive materials or at low frequencies. Throughout this paper an electrically very short dipole with three segments was used as an approximation of the Hertzian (infinitesimal) dipole. It was driven with a $1V$ voltage source and field magnitudes were scaled to fit the results from the literature. *All the results shown have been computed with the near-field* `NE` *card*, except where explicitly indicated otherwise.

The simulations were carried out on a Silicon Graphics Power Indigo2 and NEC-4 was compiled using the MIPSpro FORTRAN 77 compiler with double precision arithmetic.

Based on the result on page 107 and 109 of Maclean and Wu ([10]), the first set of tests were conducted for a short vertical electric dipole *above* the surface of the earth. The NEC-4 simulations were done for a 3 cm long electric dipole at a height of 3 cm above the surface of the earth. The simulations were carried out at frequencies of 1 MHz, 10 MHz and 100 MHz. Computations of the electric field strengths were made for heights of 3 cm and 234.8 m (800 feet) above the surface. Two sets of simulations, one for a ground conductivity, σ, of 0.01 and the other for $\sigma = 0$ were carried out. A relative permeability ϵ_r of 4 was used in both cases.

Figures 4 and 5 present a comparison of the NEC-4 results and those of Maclean and Wu. (The rather cluttered appearance of the graphs is to permit the same information to be conveyed on each graph as in the original [10].) The general agreement is quite satisfactory, except for the electric field at $f = 100$ MHz, measured near the surface of the earth (the lowermost curve in both figures). From a distance of 200 km the NEC-4 results computed with the `NE` card (near-field formulation) show a rise in the field strength, which is in contradiction with the radiation condition. The reason is the subtraction of a quasi-static term from the field due to the ground, which is then included in analytic form. Although this term should cancel with a numerically integrated $1/R^2$ term, for very large distances the cancellation fails [9]. Results are also shown in Figs. 4 and 5 for the fields computed using the `RP`

Medium	σ (S/m)	ϵ_R
Sea water	4	80
Lake water	4×10^{-3}	80
Dry earth	4×10^{-5}	4

TABLE II
VALUES OF σ AND ϵ_R USED IN THE SIMULATIONS.

card (far-field formulation); in this case, the NEC-4 results are in excellent agreement with those of Maclean and Wu.

King [2] investigated an $\hat{x}$-directed short horizontal electric dipole below the surface of earth, lake water and sea water. Some of the examples given by King have been replicated by using NEC-4. The problem considered is that of a short (1 cm long) electric dipole at a depth of 15 cm below the surface of the medium. Frequencies of 100 kHz and 10 MHz were used. Computations of the components of the electric field were carried out at a depth of 15 cm below the surface. The ρ, ϕ and z components of the electric field were calculated and are shown separately in the figures.

Table II gives the values of the conductivity, σ, and the relative permeability ϵ_r that were used in the simulations.

Figures 6, 7 and 8 shows the results at 100 kHz, while figures 9, 10 and 11 shows the results at 10 MHz. In general the agreement between the NEC-4 results and those of King are quite satisfactory. The maximum difference between the two sets of results is approximately 20 dB, while agreement between the NEC-4 and King's results are better in the far-field than close to the source. A sharp peak at 700m in figure 6 is not visible in King's results. The ripple in figure 11 is also not present in King's results; it is probably caused by the interference between waves travelling through air and ground. (The sampling may not be sufficiently fine to resolve the interference pattern smoothly). It should be accurate when NEC-4 is using the Sommerfeld/table-lookup method, but will either vanish or become inaccurate at around two wavelengths when NEC-4 starts using the approximation involving the quasi-static term discussed above [9].

V. CONCLUSIONS

Short vertical and horizontal electric dipoles near a planar interface have been modelled using NEC-4 for various representative grounds, and at frequencies of interest in the MF to VHF communication bands. The results have been compared with results from the literature for dipoles of infinitesimal length. The general comparison between the NEC-4 results and those from the monographs of Maclean and Wu [10] and King [2] was satisfactory.

Some appreciation is required by the user of the limitations of NEC-4 for problems of this type. This is especially true for source and field points located close to interfaces. Furthermore, it is important not to exceed the limitations of validity of the near-field implementation (the `NE` card in NEC-4); we have shown results where this is clearly apparent. Although this paper has not attempted an extensive validation of the far-field approximations (i.e. using the `RP` option), limitations in this regard have been elucidated — primarily the lateral wave discussed in Section III-B.

ACKNOWLEDGMENTS

We acknowledge most useful general discussions on stratified media and Sommerfeld integrals with Prof. J.H. Cloete and Dr. J.J. van Tonder of our department.

The extensive comments of an anonymous reviewer on the original submission proved most valuable, and the paper has been extensively revised, extended and corrected based on his inputs. We are most grateful for this very careful review, which clarified a number of significant issues.

Finally, we acknowledge the various parties involved in obtaining permission to release NEC-4 to the University of Stellenbosch, including the (South African) Department of Foreign Affairs and Military Attache in Washington, D.C.; the U.S. Department of the Army; Prof. D.C.Baker at the University of Pretoria (S.A.); Dr. E.K.Miller (previously at Los Alamos National Laboratory) and very importantly, G.J. Burke at Lawrence Livermore National Laboratory, whose recent responses to several queries regarding NEC-4 were also very useful.

REFERENCES

[1] B. Benhabiles, P. Lacour, M. Pellet, C. Pichot, and A. Papiernik, "A study of VLF antennas immersed in sea water: theoretical, numerical and experimental results," *IEEE Antennas Propagat. Magazine*, vol. 37, pp. 19–29, October 1996.

[2] R. W. P. King and G. S. Smith, *Antennas in Matter: Fundamentals, Theory and Applications.* Cambridge, MA.: MIT Press, 1981. Additional contributions by M.Owens and T.T.Wu.

[3] G. J. Burke, "Numerical Electromagnetics Code — NEC-4. Method of Moments. Part II: Program Description - Theory." Lawrence Livermore National Laboratory, report number UCRL-MA-109338, January 1992.

[4] G. J. Burke, "Numerical Electromagnetics Code — NEC-4. Method of Moments. Part I: User's Manual (NEC-4.1)." Lawrence Livermore National Laboratory, January 1992.

[5] G. J. Burke and E. K. Miller, "Modeling antennas near to and penetrating a lossy interface," *IEEE Trans. Antennas Propagat.*, vol. AP-32, pp. 1040–1049, October 1984.

[6] R. E. Collin, *Antennas and Radiowave Propagation.* New York: McGraw-Hill, 1985.

[7] H. d. T. Mouton, "Kommunikasie in materie." Final year project, Dept. E & E Eng, Univ. Stellenbosch (note that

this document is in Afrikaans; Eng. translation: *Communication in Matter*), November 1996.
[8] W. C. Chew, *Waves and Fields in Inhomogeneous Media*. van Nostrand Reinhold, 1990.
[9] Anonymous, "Private correspondence: comments by reviewer number 2." 1998.
[10] T. Maclean and Z. Wu, *Radiowave Propagation over Ground*. London: Chapman and Hall, 1993.

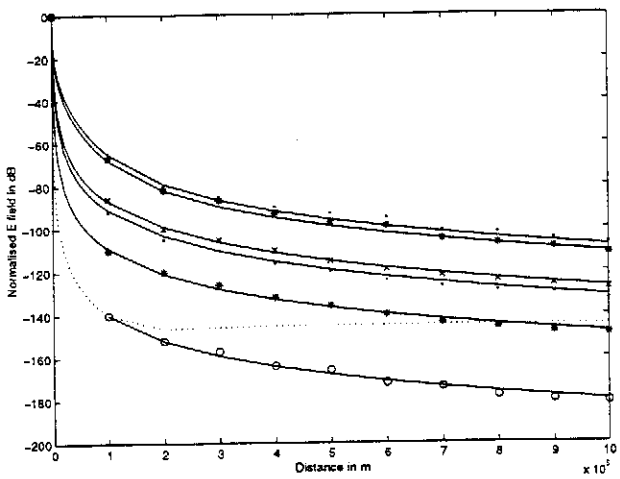

Fig. 4. The electric field strength at heights of 0m and 243.8m (800 feet) above the earth. The conductivity σ is 0.01.
Legend: uppermost curves: both f = 1MHz; above $z = 0'$; below $z = 800'$
middle upper curves: both $z = 800'$; above f = 10MHz, below f = 100MHz
middle lower curve: $z = 0'$, f = 10MHz
lowermost curve: $z = 0'$, f = 100MHz (dotted line computed using NE, solid line RP)
On all the curves, the solid lines are NEC-4 data; the symbols data from Maclean and Wu [10]. All data computed using NE except where indicated otherwise.

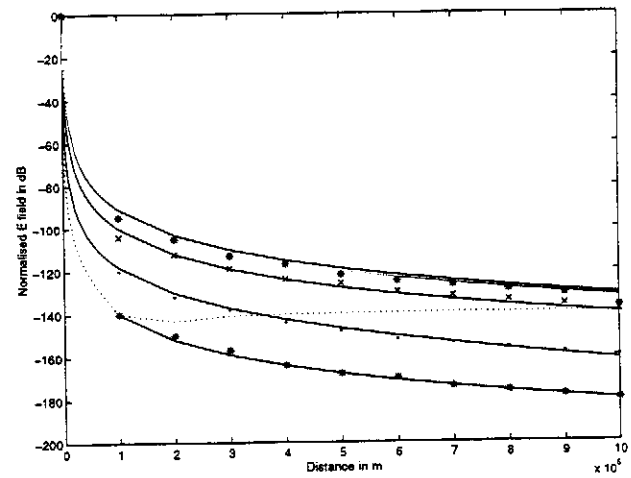

Fig. 5. The electric field strength at heights of 0m and 243.8m (800 feet) above the earth. The conductivity σ is 0.
Legend: three uppermost curves lie on top of one another; $z = 800'$ at f = 1MHz, 10MHz and $100MHz$.
middle upper curve: $z = 0'$, f = 1MHz
middle lower curve: $z = 0'$, f = 10MHz
lowermost curve: $z = 0'$, f = 100MHz (dotted line computed using NE, solid line RP))
Lines, symbols and computations as Fig. 4.

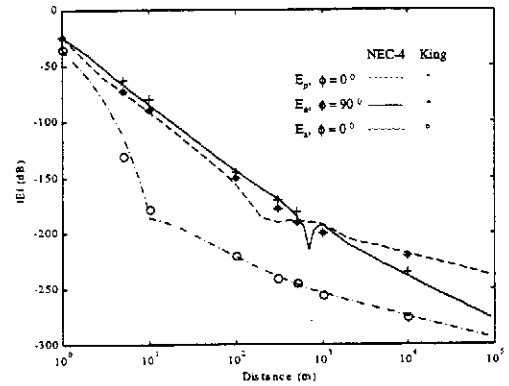

Fig. 6. The E field in sea water at 100 kHz.

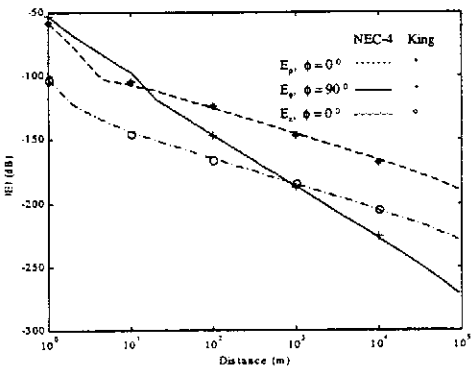

Fig. 9. The E field in sea water at 10 MHz.

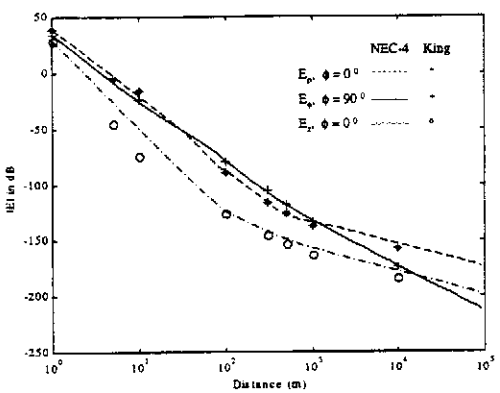

Fig. 7. The E field in lake water at 100 kHz.

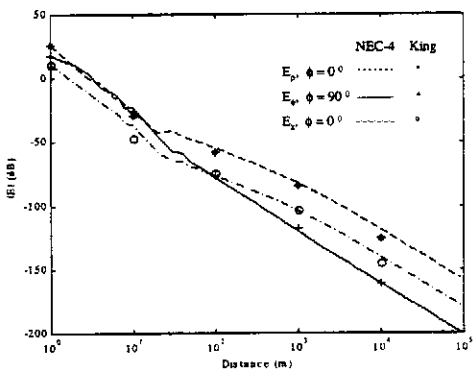

Fig. 10. The E field in lake water at 10 MHz.

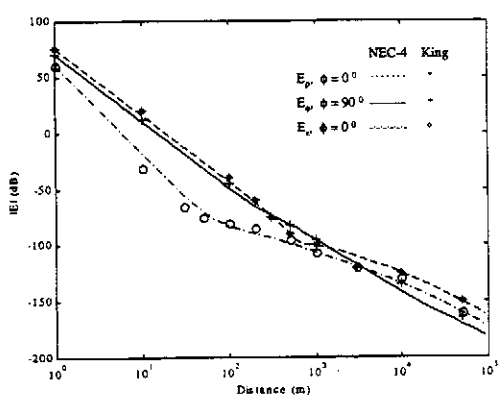

Fig. 8. The E field in dry earth at 100 kHz.

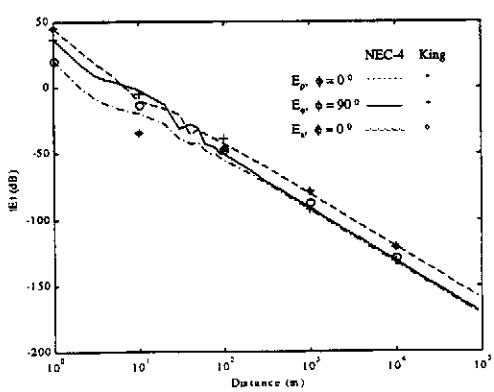

Fig. 11. The E field in dry earth at 10 MHz.